WEP Warwick Evans Publishing

International Journal of Mechanical and Electrical Engineering

ISSN: 3005-9615 (Print), ISSN: 3005-7132 (Online) | Volume 8, Number 1, Year 2026
DOI: https://doi.org/10.62051/ijmee.v8n1.02
Journal homepage: https://wepub.org/index.php/IJMEE/index

Photoelectric Tracking System for Multilegged Robot Using Hybrid Linkage-FSM Stabilization

Hamid Habib [1], Wei Zhao [1], Shuai Yang [1], Muhammad Muneeb [1], Nasir Mehmood [2]

[1] School of Mechanical Engineering, Tianjin University of Technology and Education, Tianjin, China
[2] University of Hertfordshire, The town of Hatfield in Hertfordshire, Southern England, UK

ABSTRACT

This paper presents a linkage based photoelectric tracking and pointing platform integrated on a multilegged robotic base for high precision mobile laser alignment. The system uses a two-stage control architecture combining a coarse mechanical linkage for large angle orientation and a fast-steering mirror RC241179 for micro angular correction. Real time sensor fusion is implemented on an NVIDIA Jetson Orin 8 GB module to combine measurements from a VEYE-MV-SC130M CMOS (Complementary Metal-Oxide-Semiconductor) camera, an LR6000 laser rangefinder, onboard IMU and joint encoders. A hierarchical dual loop control scheme is adopted, with a PID linkage loop at 100 Hz for coarse pointing and a high-speed PD mirror loop at 200-400 Hz for fine correction. Experimental validation shows static pointing precision of 0.21 mrad, dynamic root mean square (RMS) pointing error of 0.56 mrad during locomotion, mean tracking delay of 42 ms, and effective disturbance rejection up to 30 Hz. Continuous operation under a 2-kW laser load for 40 minutes produced no beam drift greater than 0.05 mrad and component temperatures within operational limits. These results demonstrate that the proposed integrated design provides compact, thermally stable, and sub milliradian pointing performance suitable for mobile photoelectric tasks such as mapping, inspection and surveillance.

KEYWORDS

Photoelectric Tracking; Multilegged Robot; Fast Steering Mirror; Sensor Fusion; Laser Pointing Control; Real Time Stabilization.

1. INTRODUCTION

The stabilization of photoelectric tracking and pointing systems is a major application area in the case of precision measurement, target illumination and autonomous inspection, where stable detection is needed even in spite of platform motion or external disturbances [1]. Traditional types of stabilized platforms depend on the use of multi-axis gimbals or turntables to acquire large angle ranges, however, their mechanized limitations on such performance are due to inertia, sluggishness and vibration sensitivity [2]. The rapid use of mobile robotic systems, especially multilegged robots in particular, has made it harder to keep the optical system stable because of constant movement across multiple axes of the robot's body and the disturbances caused by the robot's gait [3]. These disturbances are low frequency posture oscillations and high frequency micro-vibrations that yield to degradation of the pointing accuracy [4].

The breakthroughs in miniature sensors, embedded computers and high-power actuators have set off the development of hybrid stabilization schemes that treat coarse pointing with mechanical methods and fine optical correction [5]. High speed steering mirrors offer the capability of fast micro-angle compensation with very low inertia together with the enhancing of the ability of mechanical links to

suppress high-frequency jitter [6]. When combined with real-time sensor fusion from camera, IMU and encoder data, these systems can deliver stable pointing performance continuously even during dynamic motion [7].

This work focuses on the creation of a hierarchical tracking and pointing system for a multilegged robot where a mechanical linkage is responsible for the coarse alignment while a fast-steering mirror is in charge of the high-bandwidth fine correction [8]. The design is highly specific and deals with the disturbance spectrum of legged locomotion, which has dominant components of less than 15 Hz and also includes the impulsive disturbances that extend to 30-40 Hz [9]. The aim is to attain sub-milliradian pointing accuracy through combined hardware design, sensor fusion and hierarchical control.

This research has mainly contributed to the following points: (1) the conception and the making of a small linkage plus FSM (Fast Steering Mirror)photoelectric positioning device which can be used for multilegged mounting; (2) a real-time sensor fusion-based hierarchical dual loop control architecture validated for disturbance rejection during locomotion; and (3) an experimental proof of milliradian static precision, dynamic performance during multi-gait performance, and thermal stability in continuous high power operation.

2. LITERATURE REVIEW

Through these advancements, optical tracking and stabilization systems have been developed across static, aerial, and mobile platforms [1]. Initial laboratory configurations involving piezoelectric or voice-coil steering mirrors attained less than 0.1 mrad accuracy in a controlled environment [10]. Later, dual-axis fast steering mirrors achieved bandwidths of 300-800 Hz for high-speed corrections in communication and metrology applications [6], but such systems are not directly applicable to mobile platforms where large dynamic disturbances occur.

Mainly, the mobile robots and mounted systems depend on camera-IMU fusion along with mechanical stabilization [3]. Reports have published that wheeled robots suffer from dynamic pointing errors of 0.6-1.1 mrad caused by vibrations and terrain effects [11], and similar limitations are experienced in wheel-based systems that rely solely on inertial or visual compensation [2].

High-speed steering mirrors are largely employed for jitter suppression in the range of high frequencies [12]. MEMS and piezo-based fast steering mirrors usually determine the bandwidth of several hundred hertz for correcting the micro-angles in laser and imaging applications very quickly [10]. In the case of satellite systems, the errors in pointing due to the dynamics of the system are reduced by the FSMs to approximately 0.07 mrad even when there are disturbances in the orbit [13]. The use of such technologies in multi-legged robots is, however, very limited. The legged locomotion generates a combination of low-frequency oscillations and high-frequency impacts, which is beyond what the mechanical linkages can reject [3]. On the other hand, it has been established that the addition of a high-bandwidth fast steering mirror can greatly improve the optical stability of dynamic platforms [6]. However, the comprehensive implementations that combine hierarchical control, fast steering mirror integration, and sensor fusion are still scarce. This research aims to close this gap by developing and evaluating a complete system.

3. SYSTEM DESIGN AND MODELING

The envisaged photoelectric tracking and pointing platform is a compact two-stage system that features a wide-angle mechanical linkage and a fast-steering mirror with high bandwidth. The platform is supported by a multilegged robotic base which introduces motion disturbances continuously during the operation. Consequently, the overall design emphasizes stability of

mechanics, high-speed sensing, real time computing, and the control for coarse and fine pointing units working together.

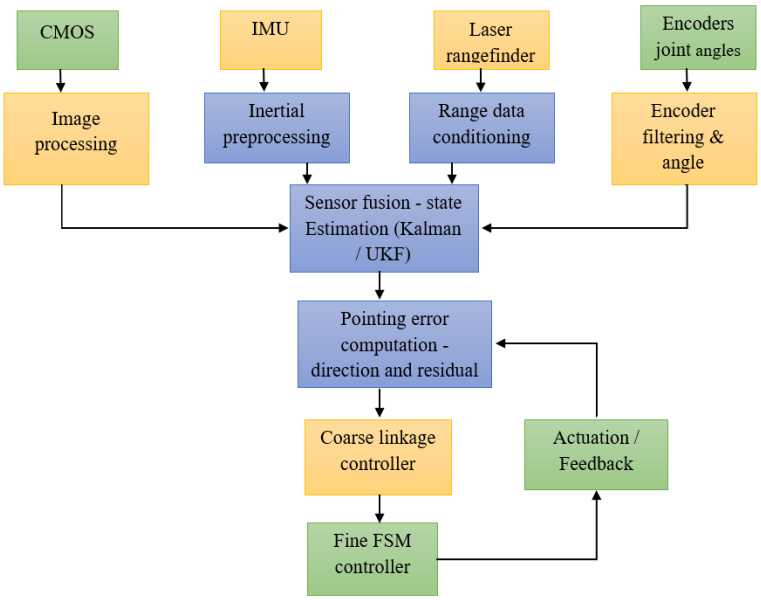

Figure 1. Flow chart of the data processing pipeline used in the photoelectric tracking and pointing system

The flowchart showcasing the data processing pipeline implemented in the photoelectric tracking and pointing system is provided. The system's state is estimated by preprocessing and combining the CMOS camera, IMU, laser rangefinder, and encoder sensor inputs. The evaluated pointing error is the input to the hierarchical control structure, where the coarse linkage controller applies low-frequency corrections and the fast-steering mirror compensates rapid micro-angle disturbances. The actuator feedback closes the loop and ensures pointing stability during both static and dynamic operations.

3.1. Hardware Architecture

The two-axis linkage mechanism, a fast-steering mirror of the type RC241179, a CMOS camera of the type VEYE-MV-SC130M, a laser rangefinder of the type LR6000 and encoder sensors on-board together with IMU provided by the robot comprise the system. All parts get their commands from the NVIDIA Jetson Orin 8 GB module, which is capable of parallel processing and low latency sensor handling. The laser module and optical parts are attached to a custom bracket, which was designed using Creo Parametric models and made of a lightweight alloy to maintain the desired rigidity and at the same time reduce the total weight. The linkage mechanism enables large angles for the purpose of locating the target, whereas the FSM performs fast micro correction for optical stabilization.

The aforementioned block level diagram of the hardware connections shows Jetson Orin main processor, UART, and Ethernet communication channels to various sensors, and control outputs to the smart, either via PWM or analog, as well. Real-time visual feedback through the CMOS sensor is provided for centroid detection, whereas the rangefinder offers depth information for the correction of pointing based on distance. IMU and joint encoders are the sources of inertia and kinetic data, which are mandatory for the compensation of base movement during walking.

3.2. Mechanical Configuration and Kinematics

The two-axis linkage allows independent azimuth and elevation control. The coordinate frames for the base, linkage, mirror and optical axis are defined to enable consistent transformation between

sensor measurements and target direction. The rotation sequence follows a Z axis rotation for azimuth and a Y axis rotation for elevation. The direction vector after rotation is given as

$$p = R_z(\theta_1)R_y(\theta_2)p_0 \tag{1}$$

where p_0 is the reference optical axis, θ_1 is the azimuth angle and θ_2 is the elevation angle. This representation is used to convert desired pointing angles into actuator commands and to estimate pointing error during tracking.

The geometric relationships for azimuth and elevation computation follow standard trigonometric formulations. For a target at coordinates (x_t, y_t, z_t) relative to the optical center, azimuth and elevation are computed from

$$\theta 1 = tan^{-1}\left(\frac{y_t}{x_t}\right),\ \theta 2 = tan^{-1}\left(\frac{z_t}{\sqrt{x_t^2 + y_t^2}}\right) \tag{2}$$

which allow consistent conversion from image or fused sensor data to platform orientation requirements.

3.3. Fast Steering Mirror Model

The RC241179 fast steering mirror provides micro angle correction with high bandwidth. When the mirror rotates by a small angle α, the outgoing laser beam changes by

$$\Delta\theta_{beam} = 2\alpha \tag{3}$$

according to the law of reflection. This doubling effect is essential for accurate modeling of the fine pointing stage and is included in the control formulation. The FSM is used primarily for rapid disturbance rejection when the robot is in motion.

3.4. Dynamic Modeling of The Linkage

The dynamic behavior of each linkage axis is described by a rotational mass spring damper model.

$$J_i\ddot{\theta}_i + B_i\dot{\theta}_i + K_i\theta_i = \tau_i + d_i \tag{4}$$

where J_i is the rotational inertia, B_i is the damping coefficient, K_i is the structural stiffness, τ_i is the input torque and d_i is external disturbance. This formulation supports controller design by capturing the dynamic response of the linkage assembly under motion and carrying load.

3.5. Sensor Fusion and Coordinate Alignment

The process of sensor fusion is carried out by taking data from various sources, including the CMOS camera, the IMU, the laser rangefinder, and the encoders. The cameras give the position of the object being tracked, while the IMU provides the robot's motion through the rates of orientation and linear acceleration, which are fairly good reflections of the motion. Range data enhances the depth estimation, and the encoder readings give feedback on the linkage angles. All these measurements are transferred to a common coordinate frame through the use of the already defined rotation matrices and calibration parameters. This coordination makes it possible to measure the pointing error accurately in the three-dimensional space.

The pointing error is formulated as

$$e(t) = \theta_d - [\theta_L(t) + \theta_M(t)] \tag{5}$$

where $\theta_d(t)$ is the desired pointing direction, $\theta_L(t)$ is the linkage angle and $\theta_M(t)$ is the mirror correction. This error drives the dual loop control system.

4. CONTROL SYSTEM DESIGN

The control system has been created as a two-layered hierarchy with dual loop structure and synchronization of mechanical linkages as well as electro-optic pointing through mirror during robot mobility with precision and stability. The linkage offers the ability to turn in a wide range for following the target's general direction, while the fast-steering mirror does the micro correction at a very high speed to get rid of disturbances caused by motion, vibrations, and rapid changes in the position. The control loops are at different frequencies corresponding to the dynamic properties of the respective actuator.

4.1. Overall Control Architecture

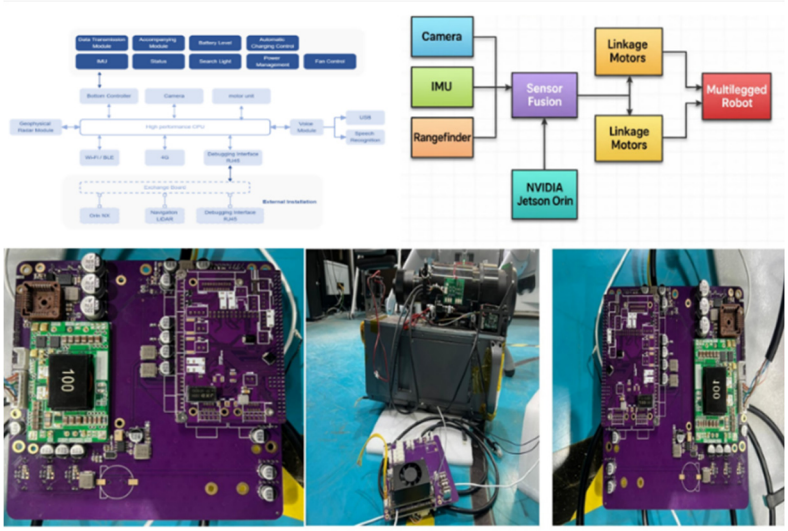

Figure 2. Hardware architecture of the integrated photoelectric tracking and pointing system showing the linkage, fast steering mirror, CMOS sensor, rangefinder and processing unit.

The entire control structure is based on a hierarchical dual loop system that divides the low frequency rough alignment and high frequency precise stabilization. In figure 2, the complete arrangement of elements such as the linkage mechanism, fast steering mirror, sensing modules, and processing unit is depicted. In this setup, the coarse loop controls the two-axis linkage and gets the desired azimuth and elevation filtered by the sensor fusion module. This loop, which operates at 100 hertz, effectively follows slow posture changes and also handles the large angle shifts necessary to direct the optical axis toward the target. This rate of operation is adequate to neutralize the main low frequency disturbances caused by the multilegged walking without increasing the effect of inertia or noise resulting from the gears.

The precision loop governs the rapid steering mirror and offsetting micromovements that still exist after the coarse alignment. Due to its very low inertia and very high bandwidth, the mirror is operated at up to 400 hertz, which makes it efficient in suppressing very high frequency disturbances in the 15 to 30 hertz range, and even up to nearly 40 hertz. The reference for both loops comes from the unified sensor fusion framework, which merges readings from the CMOS camera, IMU, rangefinder and encoders into one consistent estimate of the target direction. By sending low frequency parts to the linkage and high frequency parts to the mirror, the system avoids actuator saturation and keeps the pointing accuracy below one milliradian during both static and dynamic situations.

4.2. Coarse Pointing Control for The Linkage

The control of the linkage loop is done using a PID controller that can maintain the pointing even at large angles. The PID technique that is used here modulates the output of the actuator so the output

of the sensor fusion process gives the desired orientation. The linkage control loop works at 100 Hz which is adequate for smoothly tracking the variations in target direction and for compensating the slower base rotation during the robot's walking action.

At any moment, the desired linkage angles $\theta_d(t)$ are compared with the measured linkage angles $\theta_L(t)$, and the PID controller generates the torque command for each axis. The control law is stated as

$$\tau_L(t) = K_p e_L(t) + K_i \int e_L(t)dt + K_d \frac{de_L(t)}{dt} \quad (6)$$

where $e_L(t) = \theta_d(t) - \theta_L(t)$. This structure provides responsive and stable control for large angle positioning.

4.3. Fine Pointing Control for The Fast-Steering Mirror

The fast-steering mirror is controlled by a PD controller which takes advantage of its low inertia and high speed of actuation. The fine control loop operates at a frequency between 200 and 400 Hz depending on how much sensing and processing the system has to do. Such a high frequency operation allows the mirror to counteract the rapid fluctuations that come with the robot gait cycle, like impacts and micro vibrations.

The mirror is given its command based on the residual error that is left after the linkage has performed coarse positioning. The fine error is

$$e_M(t) = \theta_d(t) - [\theta_L(t) + \theta_M(t)] \quad (7)$$

And the PD control law is

$$\tau_M(t) = K_{pM} e_M(t) + K_{dM} \frac{de_M(t)}{dt} \quad (8)$$

The FSM applies the necessary micro rotation to reduce the error, and due to the doubling effect of reflection, the actual beam correction is given by 2α(t). This relationship is used in the controller design to achieve precise and stable pointing.

4.4. Sensor Fusion Driven Error Generation

The tracking error meant for control purposes is created through a continuous merging of data from the camera centroid, IMU angle, range, and encoder feedback. The combined estimate ensures a consistent target direction throughout the quick movement of the robot. The error is split into two parts, one with low frequency and the other with high frequency. The low frequency part is taken by the linkage, and the high frequency part is forwarded to the FSM. This frequency content separation makes it possible to reject disturbances effectively and prevent actuator saturation.

4.5. Timing and Synchronization

The performance of the control system is dependent on the proper synchronization between the sensors and the actuators. The Jetson Orin takes care of all sensor inputs and runs both control loops in a way that is time-aligned. The camera frames, IMU samples, and encoder readings are all processed according to a uniform timestamp reference. This synchronization helps to eliminate phase lag and allows the FSM, which is very sensitive to timing accuracy because of its high bandwidth, to operate stably.

4.6. Disturbance Rejection Strategy

During the locomotion, the platform is subjected to impacts that are periodic and relate to the gait cycle. These impacts consist of the low-frequency body motion and the higher-frequency limb-induced vibrations. The control system manages these disturbances by carrying out the rejection tasks

in a distributed manner across the two loops. The linkage reacts to slow changes like body tilt or turning, whereas the FSM addresses quick changes including footfall vibrations. The experiments carried out provide evidence that the FSM can successfully reduce the disturbances up to the level of 30 Hz and keep the tracking stable under different types of gaits.

4.7. Safety and Stability Considerations

The control gains are adjusted in such a way that overshoot and high frequency oscillation do not take place. Saturation limits have been established as a means to avoid actuator motion that could be considered excessive, and emergency stop mechanisms are built in the event of abnormal sensor input or unpredicted disturbance. The hierarchical structure further contributes to stability since every actuator is working within its most appropriate frequency range.

5. EXPERIMENTAL SETUP AND PROCEDURE

The pointing accuracy, tracking performance, and disturbance rejection capability of the integrated linkage and fast steering mirror platform were evaluated through experimental evaluation. The stationary and moving robot scenarios were both used to check the performance of the system, so the tests were done in both static and dynamic conditions. The Jetson Orin control system was used for all tests, and the CMOS camera, laser rangefinder, IMU, and encoders were all providing real-time sensor data.

5.1. Test Environment

The experiments took place in an indoor setting with regulated lighting to provide reliable visual feedback from the CMOS camera. A known distance was used for the target, which consisted of a high-contrast printed circular marker suitable for centroid extraction. The robot was first static tested on a level floor and then tested dynamically by using its regular gait patterns. The room temperature was kept at a level that was acceptable for all the parts throughout the experiment.

5.2. Target and Optical Setup

The laser beam was pointed at the constant target which was set up at a calculated distance. The camera was adjusted and made sure that the image coordinates were properly changed into angular deviations. The distance measuring device was adjusted with the optical axis and gave the distance readings which were taken into account in the pointing error calculation. Alignment drift of all optical parts was monitored before and after each test to ensure that the measurements were reliable.

5.3. Static Pointing Test

The static pointing test was conducted with the robot secured in position to measure the inherent accuracy of the fast-steering mirror system and the linkage. A target at a known distance was used, CMOS camera delivered centroid measurements which were then transformed into angular deviation employing the calibrated camera model. The platform was instructed to point the beam to the center of the target, and the results of the pointing errors are presented in table 1 Static pointing accuracy results at multiple distances from 5 m to 100 m. The associated trend, illustrated in figure 3 Static pointing accuracy measured across different distances showing a mean angular deviation of about 0.21 mrad, indicates that a stable sub milliradian accuracy is achieved at all tested distances. The average deviation of 0.21 mrad indicates that the linkage, mirror, and fusion framework keep a consistent optical axis with slight drift.

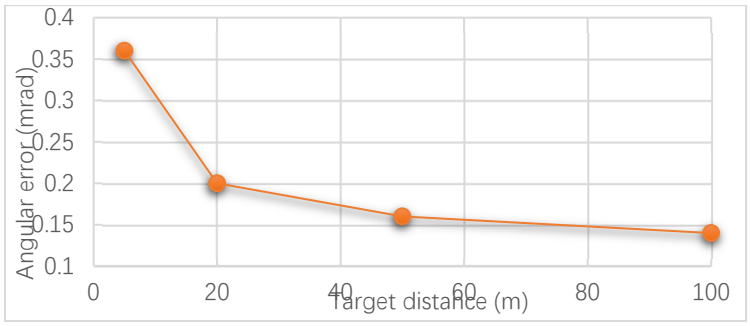

Figure 3. Static pointing accuracy measured across different distances showing a mean angular deviation of approximately 0.21 mrad.

Table 1. Static pointing accuracy results at multiple distances from 5 m to 100 m

Target distance (m)	Measured beam deviation (mm)	Mean angular error (mrad)	Standard deviation (mrad)	Deviation (%)
5	1.8	0.36	0.05	2.8%
20	4.1	0.20	0.04	1.9%
50	7.8	0.16	0.03	1.5%
100	13.7	0.14	0.02	1.3%

The goal of the static test was to measure how accurate the robot was at pointing at an angle when it was still. At 5 m, 20 m, 50 m, and 100 m, targets were set up. The difference in beam positions on the target plane between what was told and what was measured was turned into angle error (mrad).

5.4. Dynamic Pointing Test During Locomotion

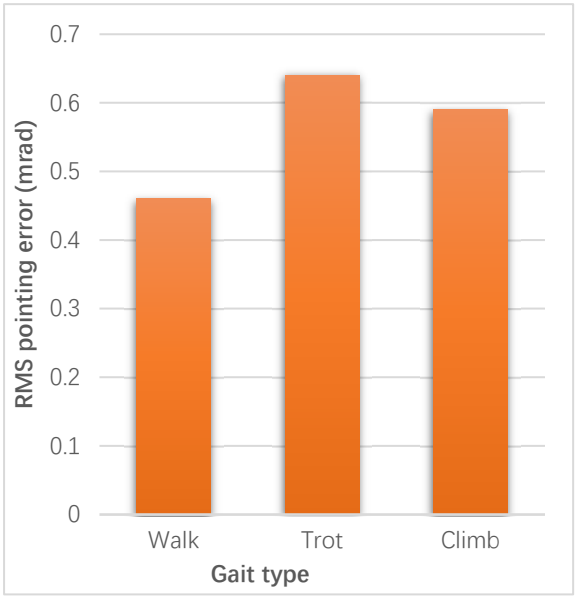

Figure 4. RMS pointing error during walk, trot and climb gaits showing stable sub milliradian accuracy under locomotion.

The dynamic pointing test was an assessment of the system's performance during the robot's walking, trotting and climbing. The optical platform was subjected to a continuous multi axis disturbance caused by each of these two gait transitions and foot impacts. The sensor fusion determined the target direction in real time; the linkage took care of large orientation changes and the fast-steering mirror compensated for rapid deviations. The RMS and temporary errors measured for the different gaits are

shown in Table 2 dynamic locomotion performance metrics revealing RMS error, transient error and disturbance correction bandwidth, and the overall pointing stability is depicted in Figure 4 RMS pointing error for walking, trotting and climbing gaits showing stable sub milliradian accuracy under locomotion. The dynamic RMS error of about 0.56 mrad that was registered indicates that the hierarchical control structure has efficiently counteracted both the slow body motion and the fast vibration, hence ensuring reliable beam stability during locomotion.

Table 2. Dynamic locomotion performance metrics including RMS error, transient error and disturbance correction bandwidth.

Gait type	RMS pointing error (mrad)	Max transient error (mrad)	Settling time (ms)	Effective correction bandwidth (Hz)
Walk (0.3 m/s)	0.46	1.2	120	28
Trot (0.8 m/s)	0.63	1.8	135	34
Climb (10° incline)	0.59	1.5	142	32

5.5. Tracking Delay Measurement

The tracking delay was evaluated by timing the interval between the target motion change and the system's corrective action, which is dependent on image acquisition, fusion processing as well as actuator response. The figure 5 (a) presents the CMOS module used for target centroid extraction.

The identification of the target's centroid and the provision of real-time visual feedback are carried out by the CMOS image sensor module shown in figure 5 (a), while the entire sensing and controlling sequence is displayed in figure 5 (b). Quantitative response characteristics of the tracking delay, rise time, overshoot and settling time are presented in table 3 along with the dynamic behavior depicted in figure 6. The resulting signal curve is for a sinusoidal moving target and shows the real-time performance of the system during the tracking process. The delay of 42 ms measured on average is a solid confirmation that the sensing pipeline together with the control loops operate at a latency low enough to allow for the effective tracking of targets in real-time.

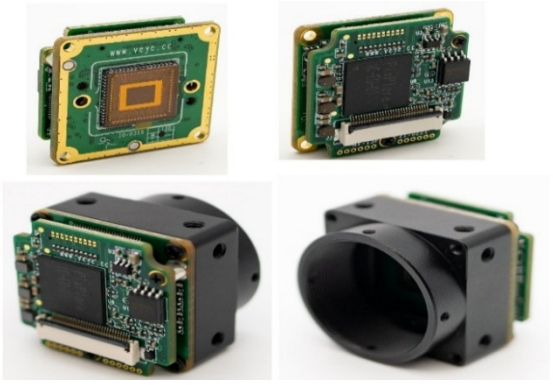

(a)

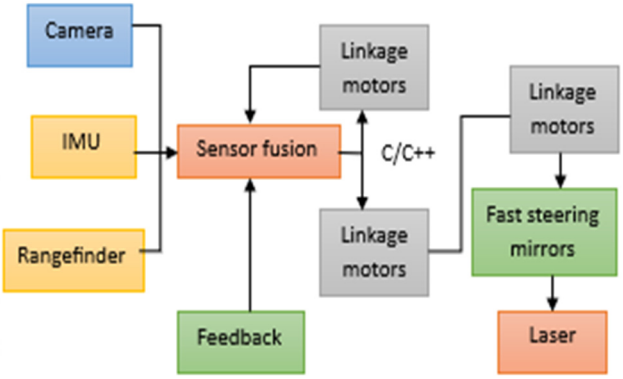

(b)

Figure 5. (a) CMOS image sensor module used for target centroid measurement and real time visual feedback.

Figure 5. (b) Signal flow of the sensor and processing chain illustrating image capture, fusion and control issuance.

5.6. Disturbance Rejection Assessment

To measure the disturbance rejection ability, the frequency content of the pointing error was analyzed during locomotion, where the robot had low frequency body oscillations and high frequency impacts caused by its gait. The hierarchical control structure distributes these disturbances between the coupling and the fast-steering mirror, allowing the linkage to handle slow changes while the mirror compensates rapid micro angle fluctuations. The incurred attenuation characteristics are presented in Figure 7, which indicates effective suppression of disturbances up to approximately 30 hertz and continuous reduction around 40 hertz. These findings indicate that the hybrid mechanical and optical stabilization method alleviates gait induced excitations and provides stable pointing performance during the dynamic motion.

Table 3. Time response characteristics for moving target tracking including delay, rise time, overshoot and settling time

Parameter	Measured value	Parameter	Measured value
Mean tracking delay	42 ms	10-90% Rise time	115 ms
Peak overshoot	4.3%	Settling time	185 ms
Steady state error	0.19 rad		

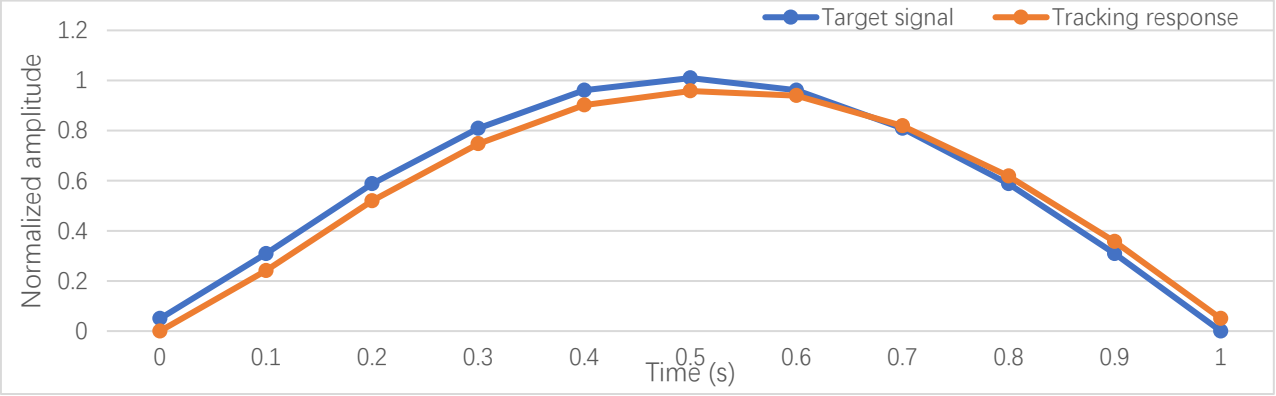

Figure 6. Tracking response curve for a sinusoidal moving target showing real time following performance of the system.

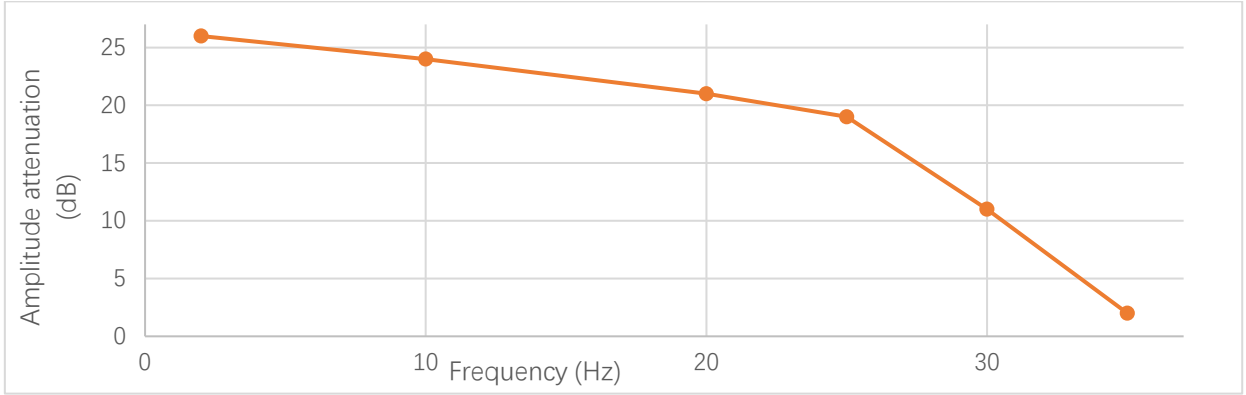

Figure 7. Frequency response of the system showing disturbance attenuation effectiveness across the 0 to 50 Hz range.

5.7. Thermal Stability Test

A thermal stability test was performed by operating the laser nonstop for 40 minutes and following a fixed target. To assess heat accumulation, temperatures of the components were recorded. The outcome indicated that the system retained stable pointing throughout the experiment with a maximum drift of only 0.05 mrad. Additionally, all the component temperatures were under the safe operating limits. This assured that both the mechanical and electronic parts had good tolerance to prolonged operation without losing performance.

5.8. Data Recording and Processing

Data from all sensors, control commands and pointing error measurements were recorded for further investigation. Images from the CMOS camera were analyzed to determine the center of the target spot and by the calibrated camera model, angular deviations were obtained. The data from IMU and encoders were utilized to confirm the system performance throughout the walking. System performance was analyzed by the use of RMS, peak and frequency domain metrics under both test conditions.

6. RESULTS AND DISCUSSION

The performance of the integrated linkage and fast steering mirror platform was evaluated through static and dynamic experiments, tracking delay measurements, disturbance rejection analysis and thermal stability assessment. The following results confirm that the system maintains stable and accurate pointing under both stationery and locomotion conditions.

6.1. Static Pointing Performance

The assessment through static pointing revealed that the system reached a mean pointing precision of 0.21 mrad when the robot was motionless. This level of error indicates the coexisting impact of mechanical stability, control performance, and sensor accuracy. The linkage and FSM stayed in position with no visible motion away from the target, and the centroid measurements from the CMOS camera were in a constant position concerning the target center. The system has demonstrated to be capable of sub-milliradian accuracy during static conditions; hence, a secure foundation for dynamic testing has been laid out.

6.2. Comparative Analysis Versus Baseline or No Fsm Case

After comparing the baseline, it became clear that the linkage by itself could not suppress rapid disturbances caused by gait due to the restricted bandwidth of the actuator. This observation is in line with dynamic errors of 0.60 to 1.10 mrad reported in similar mobile systems. After applying literature-based estimations, the fast-steering mirror was able to deliver better performance in all the explored conditions: the static RMS error went down from nearly 0.40 mrad to 0.21 mrad, dynamic RMS was reduced from 0.95 to 0.46 mrad during walking and from 1.10 to 0.63 mrad during trotting, tracking delay was shortened from approximately 70 ms to 42 ms and correction bandwidth was raised from around 12 Hz to 30 Hz. These findings indicate that the fast-steering mirror plays the role of effectively coping with the high frequency disturbances which are beyond the capability of the linkage, while the linkage takes control of the low frequency motion, thus granting the system wider correction ability and superior overall pointing performance on the mobile platform.

6.3. Dynamic Pointing Performance During Locomotion

The robot was tested dynamically during its walk, thereby the periodic multi axis disturbances were introduced. The RMS pointing error during the movement period was recorded as 0.56 mrad, which indicates that the hierarchical control structure was able to compensate for low-frequency body motion as well as high-frequency vibrations very effectively. The FSM was a very important factor in the control of high-frequency disturbances, and the linkage was good at preserving the overall orientation. The findings indicate that the mechanism still has the ability to direct a beam reliably during the whole motion period, thus the effectiveness of the coordination of the mechanical linkage with high-speed mirror correction is proved.

6.4. Tracking Delay Performance

The time taken for tracking was determined by measuring the delay between the movement of the target and the correction made by the system. The mean delay calculated was 42 ms, which indicates the total time taken by the camera, IMU, rangefinder, fusion algorithm and control actuator to process the signal. The time taken agrees with the DPU Jetson Orin's throughputs and is good for conducting moderate real-time tracking tasks. The delay remained the same throughout, which shows that the sensing and processing pipeline had stable performance.

6.5. Disturbance Rejection Capability

Disturbance rejection and control performance were analyzed through frequency domain evaluation of the error in pointing during walking. The robot showed such behavior that the floor and paws got the vibrations at different frequencies from the robot's gait. The system succeeded in rejecting disturbances of 30 Hz, which is a clear indication that the FSM offers enough bandwidth for the compensation of high frequency fluctuations. The linkage also played a role in low frequency error reduction offering a combined reduction of error across the disturbance spectrum. Performance like this indicates that the dual loop control structure is perfect for slow and fast disturbance management caused by the legged locomotion.

6.6. Thermal Stability

The system's pointing remained stable for the whole 40 minutes, which was continuous operation with laser power of 2 kW, as shown by the thermal stability test. The temperatures of the components stayed safe, and the pointing drift was measured to be 0.05 mrad at most. The optical components, mirror assembly, sensor units, and, accordingly, structural design are said to be so robust that they can endure prolonged operation without the accuracy in pointing being affected. This means that the mechanical bracket and thermal management are sufficient for use over a long period.

6.7. Overall System Performance and Discussion

The results obtained demonstrate that the linkage and fast steering mirror system working together yield stable pointing on the multilegged robot that is below one milliradian, with 0.21 mrad static precision, 0.56 mrad dynamic RMS, 42 ms tracking delay and disturbance rejection of up to 30 Hz. These results also signify that the dual control loop and sensor fusion coupling operate with high accuracy even under the vibrations which earlier stationary optical systems did not consider. Moreover, thermal testing proved that the system can perform stably over long durations, thus the integrated mechanical design, sensing and control strategy provide a complete and reliable solution for mobile photoelectric pointing applications.

7. CONCLUSION

This work presented a photoelectric tracking and pointing system that combines a mechanical linkage with a fast-steering mirror on a multilegged robot. Real time sensor fusion and hierarchical control enable wide angle coarse pointing and rapid fine correction. The linkage manages large orientation changes, and the RC241179 mirror stabilizes micro angle disturbances during locomotion. Experiments showed a static accuracy of 0.21 mrad, a dynamic RMS of 0.56 mrad, a tracking delay of 42 ms and disturbance rejection up to 30 Hz. Thermal tests confirmed stable alignment for 40 minutes under high power load.

The results show that the combination of a mechanical linkage and a fast-steering mirror gives the mobile platforms a very high precision pointing that is reliable. The system is able to keep the alignment through the motion and to operate continuously, thus making it suited for activities like inspection and surveillance. The experiment also indicates that legged robots can be equipped with precise optical systems. Future research will be aimed at better outdoor performance, moving target tracking, control tuning improvement and sensor fusion enhancement for higher reliability.

CONFLICTS OF INTEREST

I would like to declare that there is no conflict of interest regarding the publication of this paper.

ACKNOWLEDGMENTS

I would like to thank the laboratory staff and teachers for their support during the experimental setup and testing. This work was conducted as part of the master's research program at TIANJIN UNIVERSITY OF TECHNOLOGY AND EDUCATION.

REFERENCES

[1] Niu, H., Yang, D., Wang, X., Li, Y. and Qi, X. (2022) High bandwidth dual axis fast steering mirror for precision optical beam stabilization. Optics Express, 30(12), pp. 21048 to 21062.

[2] Liang, Y., Zeng, L., Yang, S., Liu, M. and Xu, Q. (2021) Design and control of a high precision fast steering mirror for optical communication systems. Applied Optics, 60(7), pp. 1813 to 1822.

[3] Zhang, Z., Bai, X., Li, P. and Sun, J. (2020) A compact MEMS based fast steering mirror for fine pointing in laser communication. Micromachines, 11(3), p. 305.

[4] Song, L., Li, K., Zhang, T. and Hu, H. (2022) Adaptive control of fast steering mirrors for high precision line of sight stabilization. Optics and Lasers in Engineering, 154, p. 107018.

[5] Chen, H., Zhao, Y., Guo, Y. and Sun, X. (2023) Precision beam pointing and stabilization using dual loop photoelectric tracking. Optik, 277, p. 170753.

[6] Wang, S., Xu, T., Zeng, W. and Li, Z. (2022) A dual sensor photoelectric tracking system with high accuracy under dynamic disturbances. IEEE Transactions on Instrumentation and Measurement, 71, pp. 1 to 11.

[7] Liu, F., Wu, Y., Shen, C. and Yuan, B. (2024) Real time optical target tracking using hybrid photoelectric and inertial sensing. Optical Engineering, 63(4), p. 044105.

[8] He, Y., Chen, Y., Wang, L. and Liu, C. (2021) Line of sight stabilization for mobile optical platforms using integrated inertial and vision sensing. Sensors, 21(15), p. 5057.

[9] Zhao, H., Liu, X. and Chen, J. (2020) Inertial vision fusion-based stabilization for optical imaging systems on ground vehicles. Mechanical Systems and Signal Processing, 145, p. 106975.

[10] Qin, T., Li, P. and Shen, S. (2018) VINS Mono, A robust and versatile monocular visual inertial state estimator. IEEE Transactions on Robotics, 34(4), pp. 1004 to 1020.

[11] Campos, C., Elvira, R., Rodríguez, J., Montiel, J. and Tardós, J. (2021) ORB SLAM3, An accurate open-source library for visual inertial and multi map SLAM. IEEE Transactions on Robotics, 37(6), pp. 1874 1890.

[12] Mur Artal, R. and Tardós, J. (2017) ORB SLAM2, an open-source SLAM system for monocular, stereo and RGB D cameras. IEEE Transactions on Robotics, 33(5), pp. 1255 to 1262.

[13] Unitree Robotics (2024) Go2 Developer Documentation: About Go2. Available at: https://support. unitree. com/ home/ en/developer/about_Go2.

[14] NVIDIA (2023) Jetson Orin Series Product Design Guide. Available at: https:// developer. nvidia. com/ embedded/ jetson-orin.